九州大学学術情報リポジトリ
Kyushu University Institutional Repository

Transient Size Analysis of Carbon Nanotube Synthesized in Diffusion Flame Environment

Muhammad Hilmi Ibrahim
School of Mechanical Engineering, Faculty of Engineering, Universiti Teknologi Malaysia

Mohd Fairus Mohd Yasin
School of Mechanical Engineering, Faculty of Engineering, Universiti Teknologi Malaysia

Muhamad Zulfan Allif Mohamad Pauzi
School of Mechanical Engineering, Faculty of Engineering, Universiti Teknologi Malaysia

Norikhwan Hamzah
School of Mechanical Engineering, Faculty of Engineering, Universiti Teknologi Malaysia

他

https://doi.org/10.5109/7172301

出版情報：Evergreen. 11 (1), pp.386-393, 2024-03. Interdisciplinary Graduate School of Engineering Sciences, Kyushu University, Japan
バージョン：
権利関係：Creative Commons Attribution 4.0 International

KYUSHU UNIVERSITY

Transient Size Analysis of Carbon Nanotube Synthesized in Diffusion Flame Environment

Muhammad Hilmi Ibrahim[1,2], Mohd Fairus Mohd Yasin[1,2,*], Muhamad Zulfan Allif Mohamad Pauzi[1,2], Norikhwan Hamzah[1,2], Mohd Zamri Mohd Yusop[3,4], Mohd 'Azizir-Rahim Mukri[3,4], Nasrat Hannah Shudin[3,4], Mohd Hanafi Ani[5], Mohd Shukur Zainol Abidin[6]

[1]School of Mechanical Engineering, Faculty of Engineering
Universiti Teknologi Malaysia 81310 UTM Johor Bahru, Johor, Malaysia

[2]High Speed Reacting Flow Laboratory (HiREF), Universiti Teknologi Malaysia, 81310 Johor Bahru, Malaysia

[3]Department of Materials, Manufacturing, and Industrial Engineering, School of Mechanical Engineering, Faculty of Engineering, Universiti Teknologi Malaysia, 81310 Johor Bahru, Malaysia

[4]Advanced Membrane Technology Research Centre Universiti Teknologi Malaysia, 81310 Johor Bahru, Malaysia

[5]Department of Manufacturing and Materials Engineering, International Islamic University Malaysia (IIUM), Kuala Lumpur, Malaysia

[6]School of Aerospace Engineering, Universiti Sains Malaysia, 14300, Penang, Malaysia

*Author to whom correspondence should be addressed:
E-mail: mohdfairus@mail.fkm.utm.my

(Received May 11, 2022; Revised March 10, 2024; Accepted March 18, 2024).

Abstract: Flame synthesis involves a complex physio-chemical process to create optimal conditions for carbon nanotube (CNT) growth. In the present study, a nickel catalyst undergoes exposure to a methane diffusion flame at various durations, with subsequent measurement of the CNT diameter. The average CNT diameter exhibits an increment until the 30-second mark, after which the diameter stabilizes at 35 nm. This growth is attributed to the nearly instantaneous occurrence of catalyst nanoparticle formation and CNT growth within the flame. The reshaping of size, crucial in determining CNT diameter, results from the aggregation-agglomeration of nanoparticle formation. The growth mechanism is partially elucidated by the vapor-liquid-solid and solvation-diffusion-precipitation mechanisms, offering insights into the governing processes.

Keywords: growth mechanism; diameter; carbon nanotubes; flame synthesis; nickel catalyst

1. Introduction

Carbon Nanotubes' (CNT) growth mechanism has been the interest of many researchers for many years to understand the basic principle of how the nanotubes grow. Although carbon fibers' formation on metal has already been realized for over a century [1)] and utilized in many applications; as recently done for denture-filler composite[2)], lubricant applications [3)], and conductive adhesive[4)]. In the early 1970s, Baker pioneered forming carbon filament on nickel, group VIII metal, and metal alloys. His works led him to propose a growth mechanism for sub-micrometer fibers, which is the fundamental explanation for CNT growth currently widely accepted [5)]. On the other hand, the vapor-liquid-solid (VLS) mechanism proposed by Wagner and Ellis on the growth of Si whisker can also be used to explain the growth mechanism of carbon filament [6–8)]. Generally, the mechanism involves three processes that include the adsorption and dissociation of carbon-containing gas precursor on the catalyst particle surface to form elementary carbon atom, the bulk dissolving of carbon atoms into nanoparticles to form a liquid metastable carbide that diffuses within the particle, and the precipitation of solid carbon at the rear side of the nanoparticles to form carbon nanofilament [9)]. Due to a vague understanding of the carbon bulk diffusion's driving force, many researchers theorized different mechanisms where the diffusion of carbon atoms would rather occur on the catalyst surfaces. This is also explained why the CNTs are hollow [1)].

In addition, Helveg provided in-situ image analysis on MWCNT grown on nickel particle and proved that the

MWCNT can grow on solid nickel particles through a mechanism involving surface diffusion of carbon species [10]. Hence, three steps vapor-solid-solid growth mechanism was proposed, which involved the dissociation of carbon precursor, the surface diffusion of carbon atoms on the catalyst particle, and the carbon precipitation in the form of nanotube growth. In another study using in-situ image analysis, Yusop et al. observed a structural change of carbon nanofiber (CNF) by agglomeration due to Joule heating of particles to form a hollow graphitic structure [11]. The effects of structural change are also observed in the annealing process of a formed carbon nanowire (CNW), which includes catalyst particle deformation and carbon nanosheet rearrangement to form carbon nanotubes when subjected to higher temperature [12]. In this case, the size of catalyst nanoparticles increases due to particle sintering, increasing the carbon diffusion and rearranging the solid core into a nanosheet of multiple walls. The transformation kinetics of the nanoparticles have been possibly affected by the annealing temperature and time [13].

In the synthesis of MWCNT, a consensus agreement of a theory that can explain its growth mechanism is still in debate[14]. This is due to the short explanation of the simultaneous nucleation and growth of several carbon walls of MWCNT. One key problem is to explain how carbon atoms diffuse and assemble to grow inner walls if the outermost wall is connected to the particle. Like SWCNTs, MWCNTs diameter still correlates with the diameter of the catalyst particle. The catalyst particle's geometry is governed mostly by the strength of the interaction between the substrate and the particle itself. In a strong particle-substrate interaction, the nanotube formation is restricted to growth via extrusion on the particle; thus, the relationship between the original catalyst particle size and CNT diameter can become, to some extent, unpredictable [15]. Some studies found that the CNT diameter is independent of catalyst particle once it exceeds a specific size resulting in catalyst particle to drop into the carbon tube.

In general, different synthesis methods play a huge role in determining the grown products' structure, quality, properties, and production. Inflame synthesis, the growth of CNT happens rapidly in a short amount of time, contrary to conventional CVD synthesis, which usually takes hours. The almost-instantaneous reaction in flame draws up a huge potential for a mass-production. The flame provides both heat and carbon supply, reducing the energy intensity required in the carbon breakup process [15–17]. CNT has been grown successfully in various flame configurations, producing various morphology and production rate [15,16,25,26,17–24]. Nevertheless, the control of flame synthesis is still facing a more significant challenge due to its complex environment. Therefore, an understanding of the essential growth mechanism that allows us to better control the synthesis is still quite crucial.

The growth of carbon nanotubes in diffusion flame can be explained generally by the VLS mechanism. However, the nanotubes' transient growth is still unable to be fully explained by the theory, especially in the synthesis where the formation of catalyst particle and CNT has grown almost instantaneously as seen in flame. In the present study, a comprehensive analysis was done on the growth of MWCNT on a nickel-based catalyst. The analysis's primary focus is to define the transient growth of the particle size and CNT diameter and their correlation towards their growth mechanisms in instantaneous reaction.

2. Experimental details

Catalyst preparation was done by titrating nickel nitrate on a silicon wafer substrate. Nickel nitrate was chosen as a catalyst precursor for its high catalytic activity when synthesizing in flame. Firstly, the 0.182g of nickel nitrate hexahydrate crystal was dissolved in 0.1-liter ethanol to get a solution of 0.1 M and kept in a reagent bottle before being sonicated for 5-10 minutes for a complete dissolve. Subsequently, the substrate was prepared. Silicon wafer disk was cut into 1 x 0.5 cm^2 and sonicated in acetone for 10 minutes. Finally, the nickel nitrate solution was drop/titrated on the prepared silicon wafer and let dried for 20 minutes at room temperature.

The CNT synthesis setup employed a laminar methane diffusion flame burner with a concentric fuel and oxidizer tubes with 17 mm and 26 mm diameter, respectively. The positioning system was installed for the localized data collection, where the substrates were placed into the flame at specific location in horizontal direction with ± 1 mm accuracy. In the experiments, the sample height above the burner (HAB) was fixed at 15 mm. The entire synthesis was done at ambient pressure in an enclosed space to minimize the entrainment of air and maintain continuous gas flow. Lab grade methane with 99.995% purity that flows in the central tube is monitored by Omron flow sensor at 0.3 slpm. Mixture of oxygen 99.9% and nitrogen 99.9% that flows in outer tube are controlled by a precision metering valve with Honeywell™ sensors, at a flow rate of 0.7 slpm and 3.0 slpm, respectively. The samples were exposed in the flame at exposure time ranging from 5 to 60 seconds.

The as-grown CNTs were examined in Field Emission Scanning Electron Microscope (FESEM) (Zeiss Crossbeam 340) and Energy Dispersive X-ray (EDX) analysis to analyze the deposited materials' morphology and elemental composition. Besides, Raman spectra analysis (HORIBA XploRA PLUS) with 532 nm wavelength laser was done at standard temperature and pressure directly on the as-grown CNTs. The images from FESEM analysis were post analyzed using Digimizer™ software to measure the grown CNTs and catalyst particles' diameter manually. The diameter measurement of one hundred unique CNT strands were recorded for every sample. The measured data were tabulated into

histogram plots for further statistical analysis.

3. Results and discussion

3.1 Characterization of carbon nanotubes

Figure 1b shows the Raman spectra of as-grown CNT from catalyst exposed for 30 s in flame under fixed condition. These conditions produce entangled CNT of different lengths but similar crystallinity which is shown by the Raman spectra with smaller D- and sharp G-band peaks. The distribution of Raman spectra at other conditions shows the consistency of CNT crystallinity regardless of exposure time in flame consistent with other studies [27]. In typical multi-walled carbon nanotubes, Raman analysis having graphitic peaks at 1550 to 1600 cm^{-1}, which correlates to the formation of CNT with high degree order and symmetry. On the other hand, the defect peak that falls in the range of 1250 to 1450 cm^{-1} is correlated to the CNT defects and disorder and G' peak falls between 2500 and 2900 cm^{-1} due to second phonon-photon response. Figure 3b shows I_D / I_G ratio of the as grown multi-walled carbon nanotubes. Respectively, all CNT that has grown at different sampling time exhibit similar I_D /I_G results. The Intensities of D-band (I_D) and G band (I_G) show a ratio I_D/I_G with a narrow range around 1.0 indicating the existence of high crystallinity tubular wall with a high degree of graphitization[28].

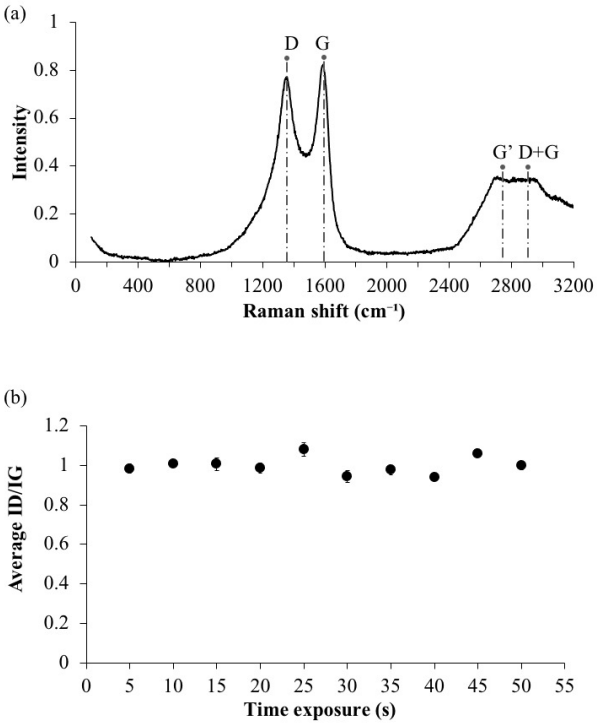

Fig. 1: (a)Raman analysis of the grown CNT. (b) The distribution of ID/IG shows the crystallinity of the grown CNT at varied exposure times.

It can be seen from Fig. 2a that dense CNT forests are formed when the catalyst is exposed to the flame. The highest CNT density form at the optimum growth region near to the flame centerline is indicated by previous work [17]. The overall density increases until the synthesized carbon nanotubes reached a uniformity in its growth. From Fig. 2b and 2c, bright spots of catalyst particle can be observed on the tip of the grown CNTs. Generally, CNTs with catalyst particle will grow along the substrate surface following a particular crystalline arrangement [29]. This mechanism is similar to well-known tip growth model explained in published literature. Catalytic particles formation on the substrate's surface happens in the high temperature environment of the flame before the carbon from hydrocarbon cracking diffused to the surface of the catalyst. The carbon atoms transport into the catalyst are driven by diffusion to continuously being stacked and forming tubes of carbon. The low magnitude force of interaction between the catalyst particle and the substrate elevates the particles during nanotube growth, creating CNTs with catalyst particles situated at the tip. In contrast, a more robust catalyst-substrate interaction force leads to CNT formation with catalyst particles positioned at the base. Despite this, the accelerated CNT growth is attributed to heightened catalytic activities. The formation of hollow tubular carbon nanotubes is a consequence of the higher diffusion rate of carbon atoms on the catalyst surface compared to bulk and/or subsurface diffusion. The increase in diameter with increasing sampling time demonstrates a rise in the catalyst involved in the reaction.

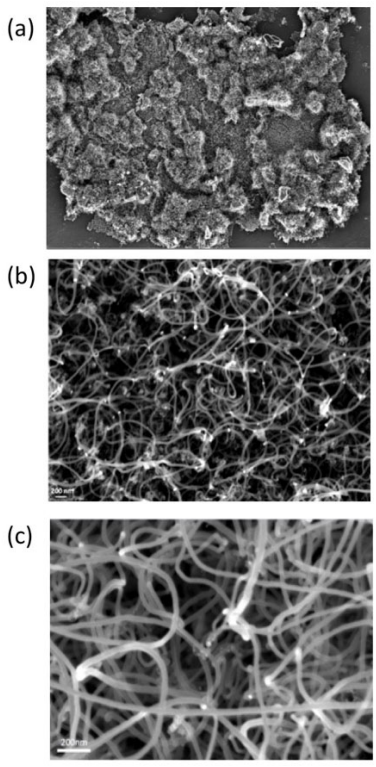

Fig. 2: FESEM images of the CNT at different magnification. (a) 1K magnification, (b) 10K magnification, and (c) 50 K magnification. Bright white spots indicate the catalyst particles

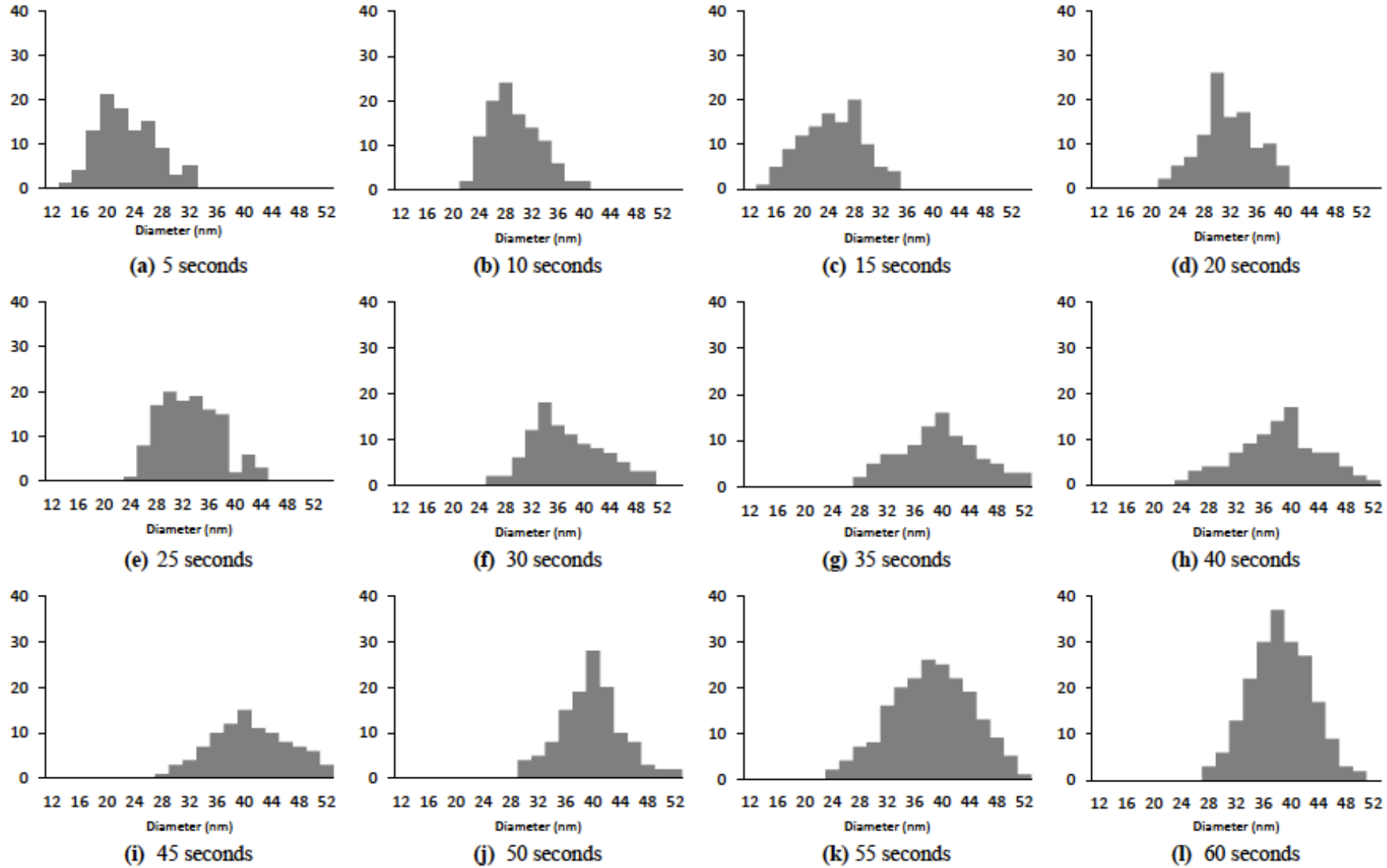

Fig. 3: CNT diameter distribution at 5 seconds increment. (a)-(f) marks the transient stage where average diameter increases while (g)-(l) shows a steady distribution of CNT diameter when exposed into flame under the same flame condition

3.2 CNT diameter distribution at various sampling time

Carbon nanotubes diameter was measured using Digimizer™ image post-processing analysis software with the statistic number of 100. The diameter distribution for sampling time up to 60 seconds with a 5-second increment is plotted in the histogram shown in Fig. 3. For shorter sampling time, the histogram tends to skew to the right indicating the presence of predominantly CNT with a smaller diameter. It also shows that the growth of CNT is rapid at this stage, with many new tubes forming at a concise duration. As the synthesis time increase to 35 seconds, the histogram started shifting towards a more normal distribution while at the same time increasing the average diameter, indicating maturity in the CNT growth process. Interestingly, the diameter distribution seems to achieve a steady distribution when the synthesis is prolonged longer than 35 seconds with an average diameter of 38 nm. The chart in Fig. 3 shows the transient growth of average CNT diameter up until 35 seconds before the distribution becomes stable. The histogram distribution agrees with previous study that found the diameter and length of CNT grow with exposure time in flame and conclude that it is due to the continuous addition of the nanotubes' concentric layer [30].

3.3 Growth mechanism of particles and CNT

According to the widely accepted VLS mechanism of CNT growth, the process involves several steps. Initially, carbon atoms subjected to high-temperature flame undergo cracking, facilitating the transformation of nickel nitrate into molten nickel. Subsequently, the nickel surface serves as the adsorption site for the free carbon. Finally, tubular carbon nanomaterials form by the diffusion and deposition of the precipitated carbon due to the grown graphene sheet's curling on the surface. This process also agrees with the Solvation-diffusion-precipitation growth mechanism proposed by Van der Waal et al [15,16]. In this mechanism, and the formation process is divided into five essential steps includes catalyst precursor decomposition, metal nanoparticle formation, decomposition and deposition of carbon on the catalyst surface, carbon diffusion into the catalyst, and carbon nanotubes nucleation-growth. The dynamics of growth is dominated by time-varying kinetics of chemical decomposition, catalytic reaction, catalyst poisoning, and molucular diffusion.

Catalyst nanoparticles are formed by the decomposition of the catalyst precursor that occurs rapidly once the fast heating reaches a sufficiently high temperature. The process involved nickel nitrate crystals decomposed and aggregated into small, nano-sized nickel particles, which serve as the basis for CNT growth [31]. Typically, the endothermic process in the decomposition of nickel nitrate hexahydrate leads to NiO formation [14]. It involves the water evaporation and dehydration, partial decomposition into intermediate species, before finally decomposing into NiO at 250-300ºC. The onset of catalytic reaction and nucleation happen at the same time by the arrangement of carbon atoms on the catalyst nanoparticles' surface, producing catalyst cap on tube tip before the lift-off. Fast heating rate from the combustion process occurs in a degree of milliseconds. Figure 4 shows the EDX after 5 seconds of sampling into the flame where the presence of nickel and carbon can already be observed. The nanoparticles' size is known to be prepared by various factors, including concentration of the solution, the quantity, the method of deposition, and annealing [32]. When sampling time is prolonged, there is a possibility of the aggregated nanoparticles to sinter into large particles via particle coalesce and migration or Ostwald ripening [33] in annealing-like environment. Kukovitsky deduced that annealing's effect produced a bigger nanoparticle, which helped deposition CNT with a bigger diameter [34]. In addition, the identical diameter of CNT produced from different initial particle sizes suggests an expansion in the size of catalyst nanoparticles during the whole process, as illustrated by Fig. 6a.

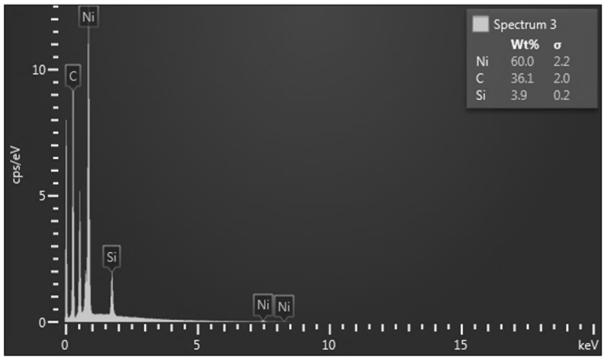

Fig. 4: EDX analysis of CNT grown at 5 seconds of sampling time. The presence of carbon (product), nickel (catalyst), and silicone (substrate) is already observed due to the rapid process.

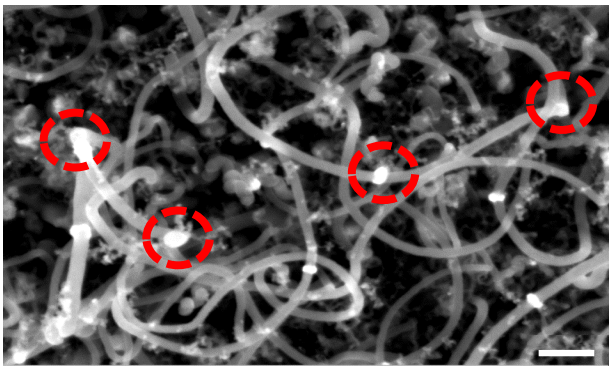

Fig. 5: Nickel catalyst is seen in the middle of CNTs strands suggesting the sintering of one particle onto another strand, forming a single long strand with multiple catalyst particles.

The particle size expansion will reach a critical size where the sintering stops due to surface tension and capillary forces from the grown CNTs, pushing the growth to be only in length. There is also a possibility that the already-grown CNTs on the particle to deposited on the exposed end of another tube, creating one single strand of

CNTs with two particles, one at the end and another in the middle, as seen in Fig. 6b and from SEM image in Fig. 5. This case is also seen in spray pyrolysis synthesis in CVD, as reported by Deck and Vecchio [31]. In a shorter sampling time, however, it is possible that the nickel nitrate does not ultimately undergo these aggregation-agglomeration-sintering processes and thus limiting the growth region on the surface of the catalyst. As a result, the active sites for CNT growth are also narrow, which produces small diameter CNTs. It is determined from the experiment that a minimum of 35 seconds of exposure in flame is needed to fully grown particles to an optimum size and produce a uniform CNT diameter. The rapid process forms rising diameter distribution, as shown in Fig. 5. Exposing a sample in flame longer than 35 seconds yields a constant CNT diameter distribution of around 38.9 nm. Nonetheless, the first 35 seconds are the essential stages to be understood to have better control over CNT flame synthesis.

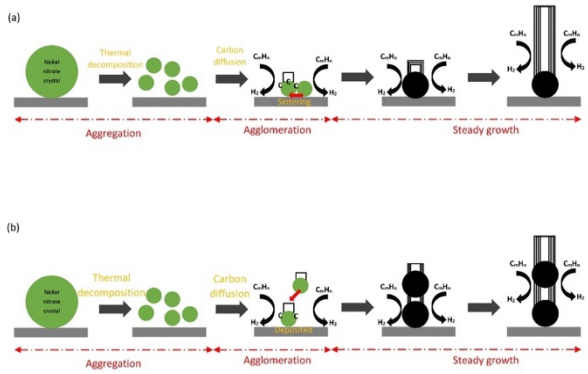

Fig. 6: Formation of catalyst nanoparticle and growth of CNT based on the aggregation-agglomeration-sintering process. (a) Particle sintering that leads to increase in particle size and carbon diffusion rate to form large nanotube diameter. (b) Particle deposited on top of another to form a long strand of CNT with multiple particles in between.

The catalyst average diameter distribution shown in Fig. 7 justifies the grown of catalyst particle size at a higher rate than the growth of CNTs. As the sample temperature rises rapidly during the flame exposure, the formation of nickel nanoparticles from nickel nitrate crystal happens instantaneously. The reduction of nickel nitrate into metal nickel nanoparticles set off at a much lower temperature. Likewise, the reduced nickel nanoparticle oxidized at a temperature of 450 ^{o}C and melted at a temperature of 600 ^{o}C. Subsequently, the formation of NiO activates a growth area for carbon deposition from the fuel stream. As a result, the growth of CNT occurs shortly after and follows the same trends as the catalyst particle counterpart. According to Lobo, nucleation grows selectively on the surface of the catalyst [35].

The nucleation may occur on the flat contact between the substrate and particles. Graphene grows laterally to the contact surface's perimeter and bend upward when the particle is grasping more carbon atoms from neighboring interstitial carbon atoms available inside the catalyst solid structure. The particle will be lifted off while the growth continues. When a new flat layer graphene nucleates on the bottom surface again, CNT with multiple layers will grow. Thus, steady growth involving absorption of carbon and diffusion of carbon into growth sites occurs. Prolonging sampling time will increase the number of carbon atoms involved in the reactions and create a longer and wider CNT. Once the absorption rate is substantially higher than diffusion, catalyst particles will encapsulate with carbon atoms and therefore stop the reaction. When the particle size has grown to a steady and uniform size at 35 seconds flame exposure and above, the grown CNT also reached its steady diameter distribution at the same time exposure. Possibly, when the active sites on the catalyst particle size are growing, rapid carbon deposition and diffusion keep adding concentric layers to the grown CNT. Smaller particle size tends to have a faster absorption rate due to the high surface to volume ratio [36]. This can be seen in rapid CNT diameter growth at sampling time up to 35 seconds. Similarly, when the catalyst particle size reached its maximum growth around 55 nm, the active sites on the particle surface only adequate to grow CNT up to certain size and thus also form the steady diameter growth distribution.

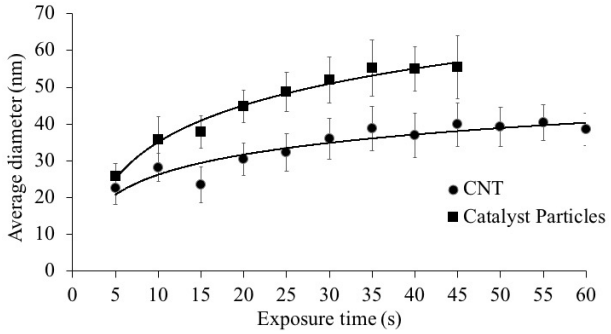

Fig. 7: The average diameter distribution for catalyst particles and CNT

Figure 8 shows the correspondence correlation between the growth of catalyst nanoparticles and carbon nanotubes when exposed to flame at different times. The CNT diameter grows within the size of particles and is not independent even when it reached ~40 nm in size, contradict the results found by Kukovitsky [34]. However, this difference is because the catalyst formation in this setup is simultaneously grown with CNT, where the entire process happens in flame exposed at a high-temperature elevation. The process indicated by the VLS and solvation-diffusion-precipitation growth mechanism require the growth of catalyst particle to occur and activate a growth site first before any deposition of carbon can be done. Thus, the one-step process resulted in the consistent growth between CNT diameter and particle size.

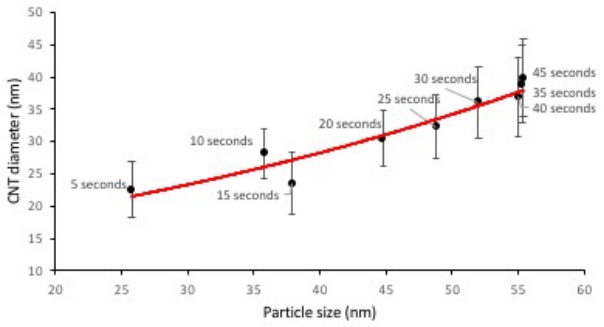

Fig. 8: Correlation between carbon nanotube diameter and catalyst particle size at various sampling times. The instantaneous reactions show that the formation of both particles reached a uniform size after 36 second sampling.

4. Conclusion

The analysis of CNT diameter is extensively studied in methane diffusion flame using the nickel-based catalyst. The purpose of the study is to investigate the transient growth of CNT and the correlation with growth mechanism. Growth mechanism that is governed by vapor-liquid-solid process generally explains the simultaneous formation of catalyst nanoparticles and CNT growth during the exposure in flame. The sampled catalyst was exposed in standing flame for duration of 5 to 60 seconds. The increase in the average diameter of CNT and catalyst particles in the transient stage from 5 to 35 seconds shows the dependencies of CNT diameter growth towards the growth of catalyst nanoparticle size over time. The completed growth of catalyst particle averaging at 55nm, also at 35 seconds resulted in the steady distribution due to the catalyst growth's maturity also reflected in the steady diameter distribution at 35 nm of the grown CNTs.

Acknowledgements

This research was supported by the Ministry of Education (MOE) through the Fundamental Research Grant Scheme (FRGS/1/2020/TK0/UTM/02/54) with cost center number R.J130000.7851.5F377.

References

1) J.-P. Tessonnier, and D.S. Su, “Recent progress on the growth mechanism of carbon nanotubes: a review.,” *ChemSusChem*, 4 (*7*) 824–847 (2011). doi:10.1002/cssc.201100175.
2) H. Sosiati, N.D.M. Yuniar, D. Saputra, and S. Hamdan, “The influence of carbon fiber content on the tensile , flexural , and thermal properties of the sisal / pmma composites,” *Evergreen*, 09 (*01*) 32–40 (2022).
3) A.C. Opia, M.K.A. Hamid, S. Samion, C.A.N. Johnson, A.B. Rahim, and M.B. Abdulrahman, “Nano-particles additives as a promising trend in tribology: a review on their fundamentals and mechanisms on friction and wear reduction,” *Evergreen*, 8 (*4*) 777–798 (2021). doi:10.5109/4742121.
4) S.H.S. Md. Fadzullah, M.M. Nasaruddin, Z. Mustafa, W.A.W.A. Rahman, G. Omar, M.A. Salim, and M.R. Mansor, “The effect of chemical surface treatment on mechanical performance of electrically conductive adhesives,” *Evergreen*, 7 (*3*) 444–451 (2020).
5) W. Wan, J. Gunning, W.J. Lee, C. Li, X. Hao, Z. Zhao, J. Qiu, and J. Patel, “The thickening of carbon fibers via a 3d island growth mechanism: new insights from a theoretical and experimental study,” *Carbon N. Y.*, 152 851–854 (2019). doi:10.1016/j.carbon.2019.06.068.
6) G. Rahman, Z. Najaf, A. Mehmood, S. Bilal, A. Shah, S. Mian, and G. Ali, “An overview of the recent progress in the synthesis and applications of carbon nanotubes,” *J. Carbon Res.*, 5 (*1*) 3 (2019). doi:10.3390/c5010003.
7) Q. Zhang, J.Q. Huang, M.Q. Zhao, W.Z. Qian, and F. Wei, “Carbon nanotube mass production: principles and processes,” *ChemSusChem*, 4 (*7*) 864–889 (2011). doi:10.1002/cssc.201100177.
8) C.-M. Seah, S.-P. Chai, and A.R. Mohamed, “Synthesis of aligned carbon nanotubes,” *Carbon N. Y.*, 49 (*14*) 4613–4635 (2011). doi:10.1016/j.carbon.2011.06.090.
9) N. Hamzah, M.F.M. Yasin, M.Z.M. Yusop, A. Saat, and N.A.M. Subha, “Rapid production of carbon nanotubes: a review on advancement in growth control and morphology manipulations of flame synthesis,” *Mater. Chem. Ahemistry A*, (2017). doi:10.1039/C7TA08668G.
10) S. Helveg, C. López-Cartes, J. Sehested, P.L. Hansen, B.S. Clausen, J.R. Rostrup-Nielsen, F. Abild-Pedersen, and J.K. Nørskov, “Atomic-scale imaging of carbon nanofibre growth,” *Nature*, 427 (*6973*) 426–429 (2004). doi:10.1038/nature02278.
11) M.Z.M. Yusop, P. Ghosh, Y. Yaakob, G. Kalita, M. Sasase, Y. Hayashi, and M. Tanemura, “In situ tem observation of fe-included carbon nanofiber: evolution of structural and electrical properties in field emission process,” *ACS Nano*, 6 (*11*) 9567–9573 (2012). doi:10.1021/nn302889e.
12) H. Pan, X. Yin, J. Xue, L. Cheng, and L. Zhang, “The microstructures, growth mechanisms and properties of carbon nanowires and nanotubes fabricated at different cvd temperatures,” *Diam. Relat. Mater.*, 72 77–86 (2017). doi:10.1016/j.diamond.2017.01.006.
13) A.A. El Mel, R. Nakamura, and C. Bittencourt, “The kirkendall effect and nanoscience: hollow nanospheres and nanotubes,” *Beilstein J. Nanotechnol.*, 6 (*1*) 1348–1361 (2015). doi:10.3762/bjnano.6.139.
14) M. Kumar, and Y. Ando, “Chemical vapor deposition of carbon nanotubes: a review on growth mechanism and mass production,” *J. Nanosci. Nanotechnol.*, 10 (*6*) 3739–3758 (2010). doi:10.1166/jnn.2010.2939.
15) H. Chu, W. Han, F. Ren, L. Xiang, Y. Wei, and C. Zhang, “Flame synthesis of carbon nanotubes on different substrates in methane diffusion flames,” *ES Energy Environ.*, 73–81 (2018).

doi:10.30919/esee8c165.

16) H. Weiwei, C. Huaqiang, Y. Yuchen, D. Shilin, and Z. Chao, "Effect of fuel structure on synthesis of carbon nanotubes in diffusion flames," *Fullerenes, Nanotub. Carbon Nanostructures*, 0 (*0*) 000 (2019). doi:10.1080/1536383X.2019.1567500.
17) N. Hamzah, M.F.M. Yasin, M.Z.M. Yusop, A. Saat, and N.A.M. Subha, "Growth region characterization of carbon nanotubes synthesis in heterogeneous flame environment with wire-based macro-image analysis," *Diam. Relat. Mater.*, 99 107500 (2019). doi:10.1016/j.diamond.2019.107500.
18) N. Hamzah, M.F.M. Yasin, M.Z.M. Yusop, M.A.S.M. Haniff, M.F. Hasan, K.F. Tamrin, and N.A.M. Subha, "Effect of fuel and oxygen concentration toward catalyst encapsulation in water-assisted flame synthesis of carbon nanotubes," *Combust. Flame*, 220 272–287 (2020). doi:10.1016/j.combustflame.2020.07.007.
19) S. Okada, H. Sugime, K. Hasegawa, T. Osawa, S. Kataoka, H. Sugiura, and S. Noda, "Flame-assisted chemical vapor deposition for continuous gas-phase synthesis of 1-nm-diameter single-wall carbon nanotubes," *Carbon N. Y.*, 138 1–7 (2018). doi:10.1016/j.carbon.2018.05.060.
20) Y. Guo, G. Zhai, Y. Ru, C. Wu, X. Jia, Y. Sun, J. Yu, Z. Kang, and B. Sun, "Effect of different catalyst preparation methods on the synthesis of carbon nanotubes with the flame pyrolysis method," *AIP Adv.*, 8 (*3*) (2018). doi:10.1063/1.5020936.
21) H. Shirae, K. Hasegawa, H. Sugime, E. Yi, R.M. Laine, and S. Noda, "Catalyst nucleation and carbon nanotube growth from flame-synthesized co-al-o nanopowders at ten-second time scale," *Carbon N. Y.*, 114 31–38 (2017). doi:10.1016/j.carbon.2016.11.075.
22) W.H. Tan, S.L. Lee, and C.T. Chong, "TEM and xrd analysis of carbon nanotubes synthesised from flame," *Key Eng. Mater.*, 723 KEM 470–475 (2017). doi:10.4028/www.scientific.net/KEM.723.470.
23) C. Zhang, B. Tian, C.T. Chong, B. Ding, L. Fan, X. Chang, and S. Hochgreb, "Synthesis of single-walled carbon nanotubes in rich hydrogen/air flames," *Mater. Chem. Phys.*, 254 (*6*) 123479 (2020). doi:10.1016/j.matchemphys.2020.123479.
24) N. Hamzah, M.F.M. Yasin, M.Z.M. Yusop, M.T. Zainal, and M.A.F. Rosli, "Identification of cnt growth region and optimum time for catalyst oxidation: experimental and modelling studies of flame synthesis," *Evergreen*, 6 (*1*) 85–91 (2019). doi:10.5109/2328409.
25) P.P.D.K. Wulan, J.A. Ningtyas, and M. Hasanah, "The effect of nickel coating on stainless steel 316 on growth of carbon nanotube from polypropylene waste," *Evergreen*, 6 (*1*) 98–102 (2019). doi:10.5109/2328411.
26) M.R. Zakaria, M.F. Omar, H.M. Akil, and M.M.A.B. Abdullah, "Study of carbon nanotubes stability in different types of solvents for electrospray deposition method," *Evergreen*, 7 (*4*) 538–543 (2020). doi:10.5109/4150473.
27) F. Xu, H. Zhao, G. Sun, and S.D. Tse, "Direct flame synthesis of carbon nanotubes on metal alloys and metal oxides," *Collect. Tech. Pap. - 44th AIAA Aerosp. Sci. Meet.*, 24 (*January*) 18208–18214 (2006). doi:10.2514/6.2006-1530.
28) D.W. Kim, H.S. Kil, K. Nakabayashi, S.H. Yoon, and J. Miyawaki, "Improvement of electric conductivity of non-graphitizable carbon material via breaking-down and merging of the microdomains," *Evergreen*, 4 (*1*) 16–20 (2017). doi:10.5109/1808307.
29) C.M. Orofeo, H. Ago, N. Yoshihara, and M. Tsuji, "Methods to horizontally align single-walled carbon nanotubes on amorphous substrate," *Micro Rev.*, 2 36–40 (2010).
30) J. Camacho, and A.R. Choudhuri, "Effects of fuel compositions on the structure and yield of flame synthesized carbon nanotubes," *Fullerenes Nanotub. Carbon Nanostructures*, 15 (*2*) 99–111 (2007). doi:10.1080/15363830601177826.
31) C.P. Deck, and K. Vecchio, "Growth mechanism of vapor phase cvd-grown multi-walled carbon nanotubes," 43 2608–2617 (2005). doi:10.1016/j.carbon.2005.05.012.
32) J. Geng, H. Li, V.B. Golovko, D.S. Shephard, D.A. Jefferson, B.F.G. Johnson, S. Hofmann, B. Kleinsorge, J. Robertson, and C. Ducati, "Nickel formate route to the growth of carbon nanotubes," *J. Phys. Chem. B*, 108 (*48*) 18446–18450 (2004). doi:10.1021/jp047898p.
33) A.T. Delariva, T.W. Hansen, S.R. Challa, and A.K. Datye, "In situ transmission electron microscopy of catalyst sintering," *J. Catal.*, 308 291–305 (2013). doi:10.1016/j.jcat.2013.08.018.
34) E.F. Kukovitsky, S.G. L'vov, N.A. Sainov, V.A. Shustov, and L.A. Chernozatonskii, "Correlation between metal catalyst particle size and carbon nanotube growth," *Chem. Phys. Lett.*, 355 (*5–6*) 497–503 (2002). doi:10.1016/S0009-2614(02)00283-X.
35) L.S. Lobo, "Nucleation and growth of carbon nanotubes and nanofibers: mechanism and catalytic geometry control," *Carbon N. Y.*, 114 411–417 (2017). doi:10.1016/j.carbon.2016.12.005.
36) M.W. Lee, M.A.S.M. Haniff, A.S. Teh, D.C.S. Bien, and S.K. Chen, "Effect of co and ni nanoparticles formation on carbon nanotubes growth via pecvd," *J. Exp. Nanosci.*, 10 (*16*) 1232–1241 (2015). doi:10.1080/17458080.2014.994679.